0090-9556/98/2605-0465–475$02.00/0
DRUG METABOLISM AND DISPOSITION
Vol. 26, No. 5
Printed in U.S.A.

HEPATIC CLEARANCE MODELS

Comparison of the Dispersion and Goresky Models in Outflow Profiles from Multiple Indicator Dilution Rat Liver Studies

ROMMEL G. TIRONA, ANDREAS J. SCHWAB, WANPING GENG, AND K. SANDY PANG

Department of Pharmaceutical Sciences, Faculty of Pharmacy (R.G.T., W.G., K.S.P.), and Department of Pharmacology, Faculty of Medicine (K.S.P.), University of Toronto, and McGill University Medical Clinic, Montreal General Hospital, McGill University (A.J.S.)

(Received November 4, 1997; accepted December 23, 1997)

This paper is available online at http://www.dmd.org

ABSTRACT:

The multiple indicator dilution (MID) technique is often used for investigation of the kinetic behavior of substrates and metabolites in eliminating organs. The present study was a systematic comparison of the utility of the Goresky model (GM) (a structural model) and the mixed-boundary dispersion model (DM) (a stochastic model) in the interpretation of influx, efflux, and removal (sequestration) coefficients, with data generated from rat liver-perfusion/MID studies. Although the GM and the DM are equivalent in their descriptions of membrane transport, they differ in their classifications of the dispersion of blood-borne elements. For the DM, the dispersion is an inverse Gaussian distribution of vascular transit times; for the GM, it is accounted for by the dispersion observed among noneliminated reference indicators (*e.g.* labeled red blood cells, albumin, sucrose, and H_2O) or the derived reference. In this study, previously published rat liver-perfusion/MID data obtained for the glutathione conjugate of bromosulfophthalein and hippuric acid, compounds that exhibit saturable carrier-mediated transport, with the GM were reanalyzed with the two-compartment DM. When the fitted values for volume and transfer coefficients were compared, good correlation was found between the fitted vascular volume for the DM and the vascular volume for the reference indicator for the GM. The influx coefficients were generally similar between the models, but improved correspondence was observed when the DM was modified to include the large-vessel transit time. In contrast, the efflux and sequestration coefficients obtained for the DM did not correspond well to those from the GM. The disagreement was due, in part, to differences in the interpretation of the late-in-time component of the reference transit time distribution curve, which was not described well by the DM. Consequently, the residence time distribution and the relative dispersion were underestimated by the DM.

There has been major progress made in the past three decades in the field of modeling of the liver for the processing of drugs and metabolites. All of the models feature the physiological determinants of clearance, *i.e.* organ blood flow, vascular and tissue binding, membrane permeability, and enzymatic activity (V_{max}) and affinity (K_M) of intracellular enzyme systems and/or excretory apparati for the removal of substrates. Several useful mathematical models that interrelate the deterministic variables have been developed to describe temporal events and, in particular, steady-state events, wherein drug and metabolite binding to liver tissue is completed and does not contribute to drug loss. Accordingly, the liver has been viewed as a well-mixed compartment ("well-mixed" model) (Rowland *et al.*, 1973; Pang and Rowland, 1977) or as an organ receiving a series of nonsegregated parallel flows surrounded by identical single sheets of hepatocytes of uniform enzymatic activity ("parallel tube" model) (Winkler *et al.*, 1973). These models have been construed as being too extreme and idealized; because there is either infinite (well-stirred model) or no (parallel tube model) mixing, they are unable to describe the asymmetrical outflow profiles or RTDs[1] observed after bolus dosing. The inadequacy has been explained on the basis of heterogeneities in flow (Miller *et al.*, 1979; Bronikowski *et al.*, 1987) and a high degree of geometric branching within the liver, which provide an intermediate mixing or dispersion. This necessitates the reselection, refinement, or development of models that could describe the observations.

The barrier-limited, distributed, capillary transit time model of Goresky (Goresky, 1963; Goresky *et al.*, 1973) and the adaptation (Roberts and Rowland, 1985, 1986) of the DM of Perl and Chinard (1968) with closed boundary conditions (Danckwerts, 1953) are such model developments. These describe curve models that resemble the outflow dilution profile observed after pulse injection, and they rec-

This work was supported by the National Institutes of Health (Grant GM38250) and the Medical Research Council of Canada (Grants MA-9104 and MT-11228). R.G.T. was supported by Graduate Research Scholarships from Merck Frosst Canada and by the Pharmaceutical Manufacturers Association of Canada-Health Research Foundation and the Medical Research Council of Canada. This work was presented, in part, at the American Association of Pharmaceutical Scientists Annual Meeting (Boston, MA) in November 1997.

Send reprint requests to: Dr. K. Sandy Pang, Faculty of Pharmacy, University of Toronto, 19 Russell Street, Toronto, Ontario, Canada M5S 2S2.

[1] Abbreviations used are: RTD, residence time distribution; RBC, red blood cell; MID, multiple indicator dilution; GM, Goresky model; DM, dispersion model; BSPGSH, bromosulfophthalein glutathione conjugate; HA, hippuric acid; MTT, mean transit time; CV^2, relative dispersion; CD, coefficient of determination; t_0, large-vessel transit time; V_B, blood volume; D_N, dispersion number; MSC, model selection criterion.

ognize that the shape and magnitude of the solute outflow concentration-time curve (the dilution profile) are complex functions of the interrelationships among blood and tissue binding, blood flow, vascular micromixing and flow heterogeneity, and cellular influx, efflux, and sequestration (metabolism or excretion). Many established principles have evolved through modeling of outflow data from experiments that encompass bolus injection of a dose containing a mixture of multiple noneliminated indicators and labeled tracer substrate; in these instances, differentiation among the injected species is enabled by the use of differential labeling and analyses (multichannel γ and β spectrometry). The kinetics of the diffusible tracer reflect those under steady-state conditions for the bulk compound, as mandated in tracer methodology. This MID technique, which was first introduced to assess the behavior of noneliminated reference substances for the understanding of liver physiology (Goresky, 1963), has become a useful experimental tool to provide mechanistic insight into the processes of transport and irreversible loss of the tracer-labeled substrate, especially in single-pass, rat liver-perfusion experiments, wherein the recirculation of solutes, which presents an added complication *in vivo*, is avoided (Wolkoff *et al.*, 1979; Schwab *et al.*, 1990; Geng *et al.*, 1995).

The GM and the mathematical formulations have a long history, first being used for descriptions of the handling of endogenous compounds by dog liver *in vivo* (Goresky *et al.*, 1973) and then being extended to analyses of xenobiotics (Schwab *et al.*, 1990; Geng *et al.*, 1995) and metabolic processing (Pang *et al.*, 1994) in perfused rat liver. The approach involves the construction of a vascular reference curve based on an initial consideration of the binding and distribution properties of the diffusible solute in the vasculature and then appraisal of the outflow curve for the labeled tracer with respect to this reference (Schwab *et al.*, 1990). In the past decade, the DM has been reintroduced and modified to describe substrate processing within the liver (Yano *et al.*, 1989, 1990, 1991; Evans *et al.*, 1991, 1993; Díaz-García *et al.*, 1992; Hussein *et al.*, 1994; Chou *et al.*, 1993, 1995; Yasui *et al.*, 1995a; Ohata *et al.*, 1996; Nishimura *et al.*, 1996; Ueda *et al.*, 1997). The model has been extended to the two-compartment DM, with recognition that the sinusoidal membrane of the liver is a transport barrier to solutes, producing compartmentalization of the vascular and cellular compartments.

Close examination of the GM and the DM reveals both similarities and differences; the models share common mathematical descriptions of cellular events such as transmembrane transfer, cellular drug metabolism, and biliary excretion (fig. 1), as first noted by Rowlett and Harris (1976). These models typically characterize cellular events by the use of influx (k_{12}), efflux (k_{21}), and sequestration (k_e) coefficients (see definitions in table 1). However, the GM and the DM differ in their descriptions of the shapes of the transit time distributions of their respective vascular reference curves.

Because of the pervasive use of both models in the interpretation of MID data to provide mechanistic insight into hepatic drug processing, there is the need to fully understand the consistency of both models with the data. The intent of this report was, therefore, to compare the ramifications of the GM and the DM to gain a better understanding of the two methods and their implications for hepatic drug processing. From a practical standpoint, it is apparent that the GM is experimentally and computationally more demanding than the DM because of the requirement for noneliminated reference indicators. We therefore became interested in assessing the similarities and differences in the analysis of dilution data by the DM compared with the GM because the solutions are more readily available, with inclusion of fewer or no reference indicators. Data that had been processed by the GM with deconvolution of the sham experiments (dilution experiments without liver) were reexamined with the DM, to allow for comparison of the two models. We compared the fitted values of the common parameters (volumes and transfer coefficients) used by the GM and the DM to describe the hepatic disposition of two compounds that are bound only to albumin and that exhibited saturable sinusoidal (carrier-mediated) transport. These compounds were BSPGSH (Geng *et al.*, 1995) and HA, the glycine conjugate of benzoate (Yoshimura *et al.*, 1998).

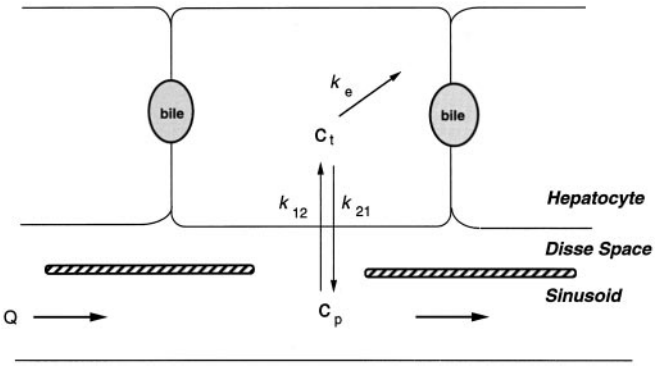

FIG. 1. *Schematic representation of solute handling at the level of a single sinusoid.*

The solute enters the liver with flow Q and is processed in a distributed-in-space fashion. At each point, drug in plasma (concentration, C_p) exchanges with that in tissue (C_t). Sinusoidal membrane transfer coefficients are denoted by k_{12} and k_{21}, the influx and efflux coefficients, respectively, whereas the cellular sequestration coefficient is represented by k_e (see table 1 for definitions).

TABLE 1

Interrelationships between influx, efflux, and sequestration coefficients for the DM and the GM and their physical equivalents

Coefficient	Coefficients for DM[a]	Coefficients for GM[b]	Physical Equivalents for GM[b]
	sec^{-1}	$ml\ sec^{-1}\ ml^{-1}$	$ml\ sec^{-1}\ ml^{-1}$
Influx	k_{12}	$f_u k_1 \theta'$ or $f_u k_1 \theta/(1+\gamma_{ref})$[c]	$f_u P_{in} S/(1+\gamma_{ref}) V_p$[d]
Efflux	k_{21}	k'_{-1} or $f_t k_{-1}$	$f_t P_{out} S/V_{cell}$[d]
Sequestration	k_e	k'_{seq} or $f_t k_{seq}$	$f_t CL_{int}/V_{cell}$[e]

[a] Transfer coefficients for the DM.
[b] Transfer coefficients for the GM and their physical equivalents.
[c] $k_1 = P_{in}S/V_{cell}$; $\theta' = \theta/(1+\gamma_{ref})$; $\theta = V_{cell}/V_p$, where V_p is the sinusoidal plasma volume and V_{cell} is the cellular water volume; $\gamma_{ref} = [f_u \gamma_{Suc} + (1-f_u)\gamma_{Alb}]$ is the apparent space ratio (interstitial/total vascular space) for total substrate; f_u is the fraction of unbound tracer within the vascular plasma space; and γ_{Alb} and γ_{Suc} are the ratios of the interstitial space to the vascular plasma water space for albumin and sucrose, respectively.
[d] $P_{in}S$ is the influx permeability cell surface area product, $P_{out}S$ is the efflux permeability cell surface area product, and f_t is the unbound fraction in tissue.
[e] CL_{int}, the hepatic intrinsic clearance for removal, equals $V_{max}/(K_m + C_{t,u})$, where V_{max} is the maximum velocity per unit of cell water, K_m is the corresponding Michaelis-Menten constant for the irreversible removal of substrate, and $C_{t,u}$ is the average unbound concentration in tissue water.

Theoretical Considerations

The GM. For the GM, a set of noneliminated reference indicators ordinarily accompanies the tracer-labeled substrate for injection into the liver. The noneliminated reference indicators include ^{51}Cr-labeled RBCs (the vascular reference, which is distributed only in the sinusoids), ^{125}I-labeled albumin and ^{14}C- or ^{3}H-labeled sucrose (which occupy the sinusoidal plasma and the interstitial or Disse space), and D_2O [a kinetic equivalent of water (Pang *et al.*, 1991) that is distributed throughout the vascular, interstitial, and accessible cellular water spaces of the organ]. The outflow concentrations are normalized to the injected dose (fractional recovery per milliliter), with observations of the progressive dispersion of labeled RBCs, albumin, sucrose, and then water, based on their increasing spaces of distribution. Another

well-known property of the model is the ability of the dilution curves for the diffusible noneliminated reference indicator to be superimposed on the labeled RBC curve, after appropriate correction of the time and the concentration for the difference in distribution volumes (Goresky, 1963). The procedure revealed the existence of a transit time delay (t_0), occurring in the nondispersing region or the large vessels, after correction for the transit times of the input and output catheters. The transit time profiles for albumin, sucrose, and water are superimposed on the RBC curve using the following relationship (Yoshimura *et al.*, 1998),

$$h_{\mathrm{Alb}}(t) \text{ or } h_{\mathrm{Suc}}(t) \text{ or } h_{\mathrm{D_2O}}(t) = \frac{1}{1+\gamma} h_{\mathrm{RBC}}\left(\frac{t-t_0}{1+\gamma} + t_0\right) \quad (1)$$

where $h(t)$ is the transfer function that describes the RTD of the reference indicator after deconvolution of the distortion caused by the inflow and outflow catheters and the injection device. The superposition procedure, when carried out by a fitting procedure, provides the optimized fitted values of t_0 and γ, a value denoting the space ratios [stationary to moving spaces, *i.e.* Disse space/sinusoidal plasma for albumin and sucrose and (cellular water + Disse space)/(sinusoidal plasma water + RBC water) for D_2O; see table 1 for definition].

The basic premise of the GM for the study of propagation of tracers is the use of vascular indicators for development of an appropriate vascular reference curve. By definition, the appropriate reference curve is the hypothetical outflow profile for a given solute that would result if the solute were neither taken up nor eliminated by the cells. Depending on the experimentally determined distribution of the solute between RBCs and plasma and on plasma protein binding, the reference curve is constructed from the combined behaviors of the labeled RBC, albumin, and sucrose curves, to illustrate the vascular distribution of the labeled tracer. For example, a tracer substrate that is neither distributed into RBCs nor bound to plasma albumin is expected to behave identically to the observed sucrose curve, in terms of the shape and the estimated vascular distribution volume. In contrast, for a drug that is very highly bound to plasma protein and is not distributed into RBCs, the vascular distribution of the reference compound is similar to that for labeled albumin. By extension, a drug that is rapidly and reversibly bound to albumin but is not bound to RBCs would have a vascular reference curve that defines a distribution space intermediate between those for sucrose and albumin. In such a situation, the reference requires the construction of the following relationship (Geng *et al.*, 1995),

$$\gamma_{\mathrm{ref}} = f_u \gamma_{\mathrm{Suc}} + (1 - f_u)\gamma_{\mathrm{Alb}} \quad (2)$$

where γ_{ref} is the apparent distribution space (interstitial/vascular space) ratio for the tracer and f_u is the unbound plasma fraction, which is defined by conventional methods such as equilibrium dialysis or ultrafiltration. Another relationship is also used when the reference is described in relation to sucrose, which is used for fitting,

$$\gamma_{\mathrm{rel}} = \frac{1+\gamma_{\mathrm{ref}}}{1+\gamma_{\mathrm{Suc}}} - 1 \quad (3)$$

where γ_{rel} is the factor that describes the appropriate interstitial space reference for the drug. The apparent volume for the reference curve (V_{ref}) is thus described with respect to that for sucrose, as

$$V_{\mathrm{ref}} = V_{\mathrm{Suc}}(1 + \gamma_{\mathrm{rel}}) \quad (4)$$

where the total volume for sucrose, V_{Suc}, can be obtained by moment analysis of the sucrose curve (catheter-corrected mean transit of sucrose × plasma flow rate).

For barrier-limited tracers, the theoretical reference transfer function may then be appropriately related to that for sucrose in describing the extracellular behavior of the labeled tracer. The organ transport function for diffusible labeled tracer can be calculated with the following equation (Yoshimura *et al.*, 1998),

$$h_{\mathrm{diff}}(t) = e^{-f_u k_1 \theta'(t-t_0)} h_{\mathrm{ref}}(t) + e^{-(k'_{-1}+k'_{\mathrm{seq}})(t-t_0)} \int_{t_0}^{t} h_{\mathrm{ref}}(\tau') e^{(-f_u k_1 \theta' + k'_{-1} + k'_{\mathrm{seq}})(\tau' - t_0)} \times \sum_{n=1}^{\infty} \frac{[(f_u k_1 \theta' k'_{-1})(\tau' - t_0)]^n (t-\tau')^{n-1}}{n!(n-1)!} d\tau' \quad (5)$$

where θ is the ratio of the cellular water space (V_{cell}) to the sinusoidal plasma space (V_p) and θ' is $\theta/(1 + \gamma_{\mathrm{ref}})$, with parameters describing the rate coefficients for influx ($f_u k_1 \theta'$), efflux (k'_{-1}), and sequestration (k'_{seq}) (see definitions in table 1). The fitting procedure furnishes estimates of γ_{rel} and the rate coefficients. These, in turn, provide the influx and efflux rate constants (k_1 and k_{-1}, respectively), as defined by Goresky and co-workers (Goresky *et al.*, 1973; Geng *et al.*, 1995; Yoshimura *et al.*, 1998), and the permeability surface area products for influx and efflux across the hepatocyte membrane (table 1). The first term of eq. 5 represents the throughput component or material that propagates through the system, *i.e.* the portion of the tracer that passes through the liver without entering parenchymal cells; this throughput component is obtained from eq. 5 by setting k'_{-1} to 0. The second term represents material that enters the liver cell and later returns to the vascular compartment, or the returning component; this is given by the difference between the total outflow profile and the throughput component.

The DM. The DM conceptualizes that the blood flowing through a labyrinth of ramified interconnecting sinusoids is nonideal and causes a dispersion of noneliminated and eliminated substances (Roberts and Rowland, 1985, 1986). There are two parameters that characterize the model, *i.e.* D_{N}, or the inverse of the Peclet number, which describes the degree of mixing or dispersion resulting from heterogeneous blood flow through the microvasculature, and the efficiency number, R_N, or the term for removal

$$R_{\mathrm{N}} = \frac{f_u CL_{\mathrm{int}} \rho}{Q} \quad (6)$$

where f_u is the unbound fraction, CL_{int} is the intrinsic clearance or the inherent ability for removal of the unbound substrate, and ρ, as defined in earlier publications (Roberts and Rowland, 1985, 1986), is given by $P/(P + CL_{\mathrm{int}})$, where P is the permeability. The use of $\rho = 1$ is justified when permeabilities far exceed the intrinsic clearance.

The dispersion observed in the outflow dilution profile for a given solute is modeled with a second-order partial differential equation that can be described in Laplace transformations after delineation of the boundary conditions. In general, the mixed-boundary DM (Roberts *et al.*, 1988) is preferred over the closed-boundary DM of Perl and Chinard (1968) (Danckwerts, 1953; Roberts *et al.*, 1988) because of the ease of calculation in the former. The frequency output of a solute can be presented in the Laplace domain (Evans *et al.*, 1991),

$$f(s) = w(s)_{\mathrm{H}} \cdot w(s)_{\mathrm{NH}} \quad (7)$$

where s is the Laplace operator and $w(s)_{\mathrm{H}}$ and $w(s)_{\mathrm{NH}}$ are the transfer functions that describe the spread of solute by passage through the hepatic and nonhepatic (inflow and outflow catheters, tubing, and devices) regions, respectively. The transfer function of the frequency

output, $f(t)$ or $QC(t)$/dose, in the absence of the liver can be described by (Evans *et al.*, 1991)

$$w(s)_{NH} = \exp\left(\frac{1 - \sqrt{1 + 4D_{N,NH}MTT_{NH}s}}{2D_{N,NH}}\right) \quad (8)$$

where $D_{N,NH}$ is the nonhepatic D_N and MTT_{NH} is the MTT of the reference in the sham experiment (volume of nonhepatic portion/flow or V_{NH}/Q).

The $w(s)_H$ value, or hepatic transport function of the solute, may be calculated for the one- or two-compartment DMs. The one-compartment DM is used to describe the processing of solutes that establish rapid equilibration between the vasculature and the cells. For the noneliminated reference, which is not removed, the weighting function is

$$w(s)_{H,ref} = \exp\left(\frac{1 - \sqrt{1 + 4D_N V_B s/Q}}{2D_N}\right) \quad (9)$$

where V_B is commonly considered as the volume of the distribution for the noneliminated reference compound in the central compartment and is the sum of the vascular volume and the Disse space for albumin or sucrose and Q is the perfusate flow rate (Evans *et al.*, 1991). For a solute that is removed in the one-compartment model (Roberts and Rowland, 1986), the following weighting function applies,

$$w(s)_H = \exp\left[\frac{1 - \sqrt{1 + (4D_N/Q)(V_B s + \rho f_u CL_{int})}}{2D_N}\right] \quad (10)$$

where V_B is the extracellular volume (combined sinusoidal and Disse spaces) and CL_{int} is the intrinsic clearance for removal of unbound substrate.

However, with recognition that the hepatocyte membrane is a barrier that facilitates or retards the entry of solutes, producing different concentrations in the vasculature and cells, the two-compartment model has been developed for the description (Yano *et al.*, 1989). Elimination from the vascular (Yano *et al.*, 1990, 1991) and/or peripheral (Yano *et al.*, 1989; Evans *et al.*, 1991, 1993) compartments has been considered. With the assumption that the vascular and cellular compartments are physiological spaces that are equivalent to the central and peripheral compartments, respectively, which are separated by the hepatocyte membrane, cellular removal likely occurs in the peripheral compartment. Under these circumstances, the weighting function for a solute that is distributed between the extracellular and cellular regions in liver is described as follows (Evans *et al.*, 1991),

$$w(s)_H = \exp\left[\frac{1 - \sqrt{1 + (4D_N \cdot V_B/Q)[s + k_{12} - k_{12} \cdot k_{21}/(s + k_{12} + k_e)]}}{2D_N}\right] \quad (11)$$

where V_B is commonly considered the extracellular volume (combined vascular and Disse spaces) and k_{12}, k_{21}, and k_e are the influx, efflux, and elimination coefficients, respectively (fig. 1 and table 1).

For the DM, the curve form of the vascular reference is a modified inverse Gaussian distribution, and the same function identifies the curve profile for the vascular reference. The curve form differs from that for the GM, which is constructed from the noneliminated references. For the DM, the V_B, the combined volume of the extracellular spaces (vascular volume + Disse space), is equivalent to the vascular volume of distribution for the reference in the GM. For the DM, the rate coefficients have been defined with respect to the compartment wherein the flux originates and have not been corrected for binding; for the GM, all of the rate constants are defined with respect to the accessible cellular water space (V_{cell}), and the permeability surface area products have been corrected for protein binding (table 1). As in the GM, the throughput component for the DM can be obtained by setting k_{21} to 0, and the corresponding hypothetical reference curve can be determined by setting the influx parameter, k_{12}, to 0 (Evans *et al.*, 1993). Again, the difference between the total outflow profile and the throughput component yields the returning component. For the DM, the transit time of the noncapillary vessels (t_0) has not been previously considered. The absence of this delay factor in the DM might simply have been an oversight, or the factor might have been viewed as being unimportant in the distortion of the impulse. In contrast, the GM describes the large vessels as a nonexchanging and nondispersing region characterized by its transit time, t_0.

Materials and Methods

Data Set. Data from single-pass, rat liver-perfusion/MID experiments were used in the present analysis. The data had been previously analyzed using the GM. In the first set of studies ($N = 12$), a bolus injection of [^{3}H]BSPGSH was introduced simultaneously with the reference indicators (^{51}Cr-labeled RBCs, ^{125}I-albumin, [^{14}C]sucrose, and D_2O) (Geng *et al.*, 1995), under steady-state conditions, with various concentrations of BSPGSH (20–214 μM). Similarly, in another set of studies ($N = 19$), [^{3}H]HA was injected, together with the set of noneliminated reference indicators, with a background concentration of HA (1–930 μM), under steady-state conditions, with or without the presence of lactate (20 mM) or benzoate (10–873 μM), compounds that were found to inhibit HA uptake (Yoshimura *et al.*, 1998). The outflow of [^{3}H]BSPGSH or [^{3}H]HA was expressed as the fraction of the administered dose eluting per second [$C(t)$/dose] or as the frequency output [$f(t)$ or $C(t)Q$/dose].

Data Analysis. The frequency output was analyzed according to the DM (Evans *et al.*, 1991). Data from sham experiments, in which labeled RBCs were injected into the inflow and outflow catheters, were used to evaluate $w(s)_{NH}$ (eq. 8). Preliminary fits indicated that eq. 8 was unable to describe the observed exponentially multiphasic decline in the sham experiments. Therefore, $w(s)_{NH}$ was empirically fitted to the two-compartment DM for noneliminated references where there is no elimination

$$w(s)_{NH} = \exp\left[\frac{1 - \sqrt{1 + (4D_{N,NH} \cdot V_{NH}/Q)[s + k_{56} - k_{56} \cdot k_{65}/(s + k_{65})]}}{2D_{N,NH}}\right] \quad (12)$$

where $D_{N,NH}$ is the nonhepatic D_N, V_{NH} is the volume of the nonhepatic experimental system, Q is the perfusate flow rate, and k_{56} and k_{65} are the parameters accounting for the biphasic decline. Least-squares fitting of the sham experiment data to eq. 12 yielded estimates of 0.0163, 1.04 ml, 0.105 sec^{-1}, and 0.388 sec^{-1} for $D_{N,NH}$, V_{NH}, k_{56}, and k_{65}, respectively.

Because we had previously demonstrated that both BSPGSH and HA exhibit barrier limitation (carrier-mediated saturable uptake processes), the hepatic transfer function, $w(s)_H$, for the two-compartment DM (eq. 11) was used. Since only hepatic uptake and efflux occur for HA, the hepatic transport function in eq. 11 was modified by setting $k_e = 0$.

Further analysis of the outflow data was performed, in which the DM included a lag time, t_0, that characterizes the hepatic large-vessel transit time of the GM. The t_0 was obtained either from the GM or from the fitting procedure. In these analyses, the frequency output was described by the following equation in the Laplace domain,

$$f(s) = w(s)_H \cdot \exp(-t_0 \cdot s) \cdot w(s)_{NH} \quad (13)$$

The MTT and the CV^2 of the diffusible tracers were estimated for the DM according to the equations provided by Yano *et al.* (1989). The MTTs and variances from the GM were obtained by integration of the model functions with 1000 points using the trapezoid rule, with or without monoexponential extrapolation. The number of points was large enough that there should be no problem with accuracy. From these, correction of the MTTs and CV^2 for the catheter was made.

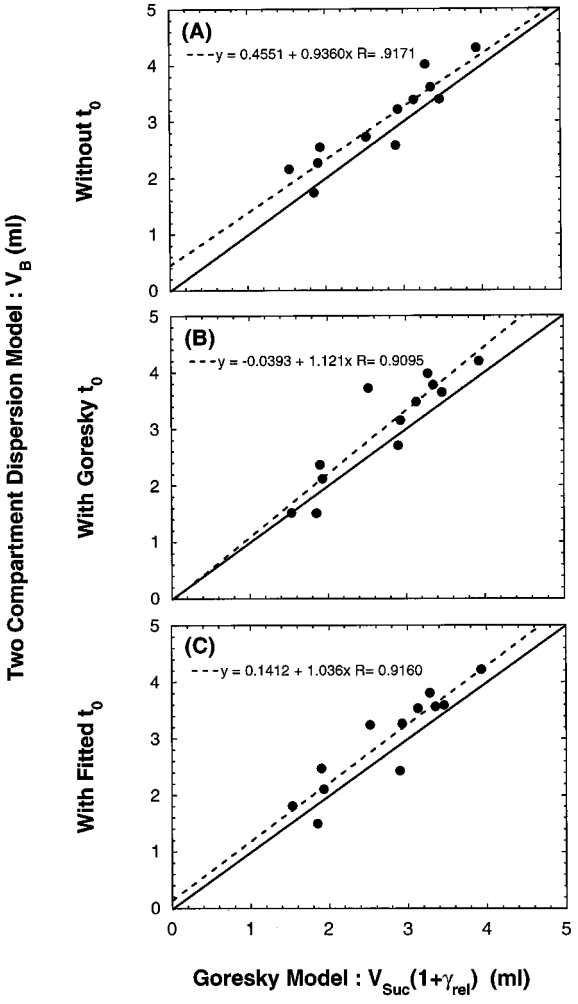

FIG. 2. *Relationship between the vascular volume (V_B) of the DM and the volume for the reference [$V_{Suc}(1 + \gamma_{rel})$] of the GM for sets A, B, and C for BSPGSH (data from Geng et al., 1995).*

The *dashed lines* were established by linear regression (equations shown, with correlation coefficients, R), whereas the *solid lines* are the lines of identity.

Fitting. The frequency outputs were fitted to eq. 7 or 13 with the use of a weighted least-squares minimization procedure, using a Levenberg-Marquardt algorithm, found in the program SCIENTIST (Micromath Scientific Software, Salt Lake City, UT). Numerical inversion of the Laplace transforms was accomplished using the Piessens-Huysmans algorithm used by the program. All parameters (D_N, V_B, the transfer coefficients, and, where appropriate, t_0) were estimated during the fitting procedure with the weighting chosen at 1/observed value. For each experiment, the frequency output data were modeled with the two-compartment DM without inclusion of t_0 (set A), with t_0 obtained from GM (set B), and with fitted t_0 (set C).

Statistical Analysis. All data are presented as mean ± SD. The paired *t* statistic was used for the comparison of paired data of sets A or C of the DM with those of the GM. Data of set A were compared with those of set C, because these are data fits of the DM with and without t_0, respectively. The MSC (SCIENTIST for Windows manual; Micromath Scientific Software), a modified Akaike information criterion, was used to compare the goodness of fit to the model; a larger value for MSC suggests a superior model.

Results

BSPGSH Data. Good correlation was obtained between the estimated apparent V_B from sets A, B, and C in the DM and the vascular volume for the reference in the GM ($R > 0.90$) (fig. 2 and table 2). However, these values (approximately 3–3.4 ml) were significantly greater than the volume for the vascular reference according to the GM (2.7–3 ml). Similarly, an excellent correlation ($R > 0.91$) was found between the influx coefficients determined by the DM (k_{12}) and those determined by the GM ($f_u k_1 \theta'$) (fig. 3). Paired analysis of the k_{12} values estimated in sets A, B, and C failed to show differences between the DM and the GM ($p > 0.05$) (table 2), although clearly the correlation improved with inclusion of t_0 (fig. 3). In contrast, values for k_{21} and k_e obtained for the DM did not correspond well to the respective efflux and sequestration coefficients obtained from the GM (figs. 4 and 5 and table 2). The DM values for k_{21} and k_e were higher than those from the GM (set C compared with set A, $p < 0.01$) (table 2). The addition of t_0 to the DM improved the correlation between the respective parameters k_{21} and k_e (compare fig. 4*A* with fig. 4, *B* and *C*, and compare fig. 5*A* with fig. 5, *B* and *C*) and increased D_N significantly (almost 3-fold) (table 2).

The fit of the BSPGSH outflow curve according to the DM was further explored by simulation of the reference curves (fig. 6*A*) with the fitted parameters for D_N and V_B for set C (see example, at a BSPGSH concentration of 214 μM) and was compared with that of the GM. For the GM, the reference curve fell between that of labeled sucrose and labeled albumin, because there is substantial binding of BSPGSH to albumin (unbound fraction = 0.1); the reference curve decayed slightly faster than the sucrose curve. However, for the DM, the downslope of the reference curve decayed much more rapidly. The predicted throughput component for the DM was much smaller than that for the GM; consequently, the returning component was greater (fig. 6*B*). All of these discrepancies existed even though the fit of the data to the GM was only marginally better than that for the DM.

HA Data. Fitting was successful for all experimental data in sets A and C. However, convergence was obtained for only 14 of the 19 experiments in set B, because of the unexpectedly large t_0 obtained with the GM. Hence, data from only the 14 experiments were reported among all data sets. The estimates of V_B for sets A, B, and C correlated well with the volume for the reference determined by the GM (3.0 ± 0.5 ml) (fig. 7 and table 2). The k_{12} of the DM was moderately correlated with the influx coefficient of the GM in sets A and C (fig. 8). Inclusion of t_0 in the DM did not improve the correspondence for k_{12} between the DM and GM estimates (compare fig. 8*A* with fig. 8, *B* and *C*). However, improved correspondence in the efflux parameter (k_{21}) was observed for sets B and C with GM values when t_0 was included in the DM (compare fig. 9*A* with fig. 9, *B* and *C*). Again, a significant increase of the D_N value was observed with the inclusion of t_0 (table 2).

A representative fit of the indicator dilution profile for [^{3}H]HA (930 μM) is shown in fig. 10. For the GM, the reference curve closely followed that for sucrose (fig. 10*A*), owing to the modest unbound fraction of HA in plasma (unbound fraction = 0.54). The reference curve for the DM lay close to the sucrose curve at early time points and then decayed in a monoexponential fashion. The model fit to the [^{3}H]HA data was similar for the GM and the DM, although the GM tended to describe the late-in-time data better (fig. 10*B*). For [^{3}H]HA, the DM estimated a greater throughput and thus a smaller returning component, compared with the GM.

The MTT for BSPGSH estimated with the DM was significantly smaller than that from the GM; however, similar values were found for HA (table 3). Values for CV^2 were generally lower for the DM than for the GM; however, significance was found only for HA and not BSPGSH.

Discussion

In this report, we compared the fitted values for the common parameters that characterize the hepatic disposition of two solutes

TABLE 2

Summary of fitted parameters from the DM (set A, DM without t_0; set B, DM with GM t_0; set C, DM with fitted t_0) and the GM

Solute	Parameter							Goodness of Fit Criteria	
	D_N	V_B		t_0	k_{12}	k_{21}	k_e	CD	MSC
		ml	*% liver weight*	*sec*	*sec*$^{-1}$	*sec*$^{-1}$	*sec*$^{-1}$		
BSPGSH (13 ± 2 g liver)									
GM	NA[a]	2.7 ± 0.8	21 ± 6	4.1 ± 1.1	0.08 ± 0.05	0.005 ± 0.004	0.029 ± 0.012	NA	NA
DM set A	0.04 ± 0.01	3.0 ± 0.8[b]	23 ± 7[b]	0	0.08 ± 0.03	0.033 ± 0.017[b]	0.055 ± 0.009[b]	0.98 ± 0.01	4.05 ± 0.73
DM set B	0.19 ± 0.09[c]	3.0 ± 0.9[b]	23 ± 7[b]	4.1 ± 1.1	0.08 ± 0.05	0.013 ± 0.008[b,c]	0.041 ± 0.010[b,c]	NA	NA
DM set C	0.16 ± 0.08[d]	3.0 ± 0.9[b]	23 ± 7[b]	3.6 ± 1.2	0.08 ± 0.04	0.013 ± 0.007[b,d]	0.041 ± 0.008[b,d]	0.99 ± 0.01[d]	4.86 ± 0.85[d]
HA (11 ± 1.3 g liver)									
GM	NA	3.0 ± 0.5	27 ± 4	4.3 ± 1.1	0.063 ± 0.023	0.091 ± 0.026	0	NA	NA
DM set A	0.08 ± 0.05	2.9 ± 0.5	26 ± 5	0	0.069 ± 0.024	0.073 ± 0.016[b]	0	0.98 ± 0.01	3.97 ± 0.62
DM set B	0.43 ± 0.16[c]	3.4 ± 0.7[b,c]	30 ± 5[b,c]	4.3 ± 1.1	0.066 ± 0.069	0.107 ± 0.048[c]	0	NA	NA
DM set C	0.18 ± 0.09[d]	3.0 ± 0.5	27 ± 4	2.2 ± 1.2[b]	0.056 ± 0.018[b,d]	0.073 ± 0.022[b]	0	0.99 ± 0.01[d]	4.44 ± 0.86[d]

[a] NA, not applicable.
[b] Significantly different from data from the GM ($p < 0.05$, paired t test).
[c] Set B significantly different from set A ($p < 0.05$, paired t test).
[d] Set C significantly different from set A ($p < 0.05$, paired t test).

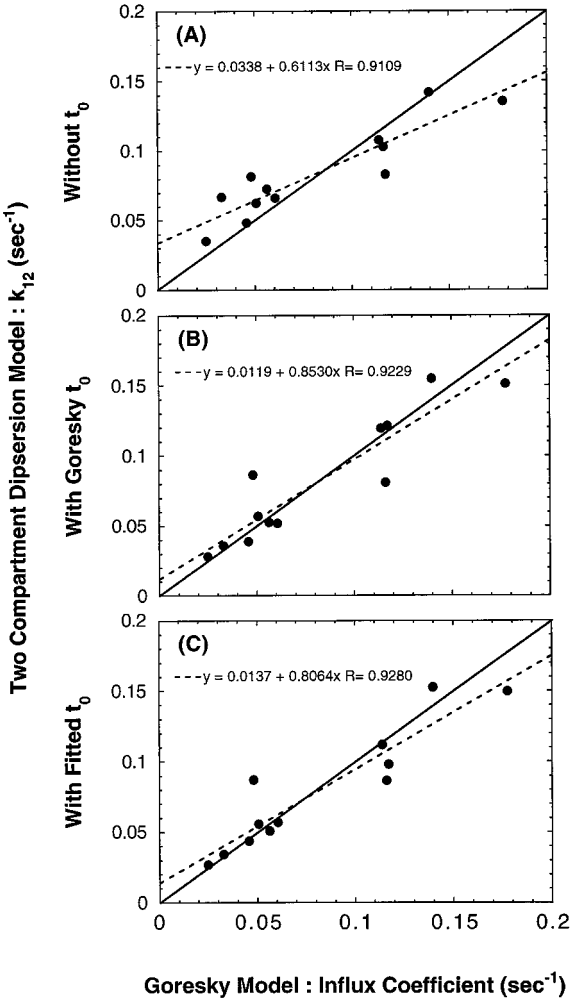

FIG. 3. *Relationship between influx coefficients (k_{12}) determined by the DM and the GM for BSPGSH (data from Geng et al., 1995).*

The *dashed lines* were established by linear regression (equations shown, with correlation coefficients, R), whereas the *solid lines* are the lines of identity.

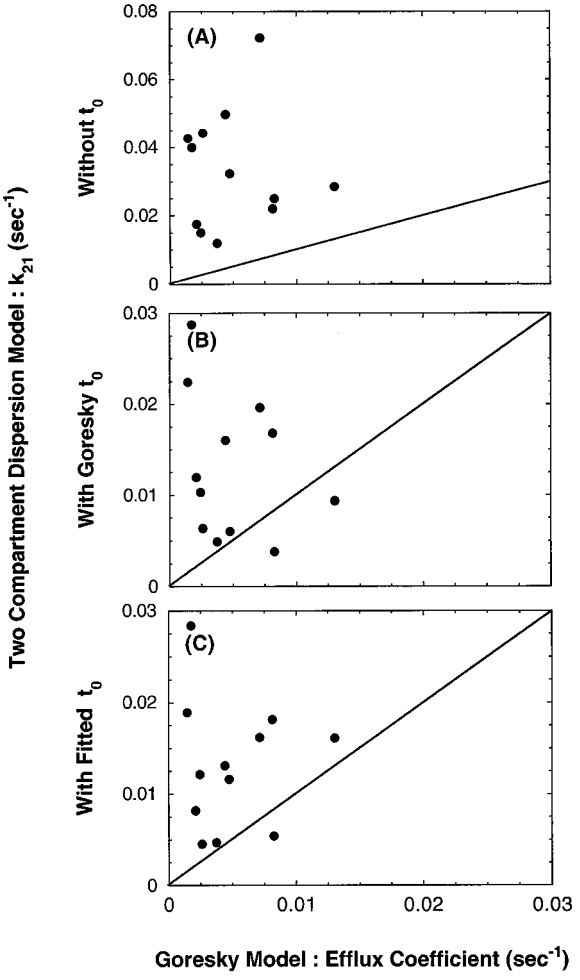

FIG. 4. *Relationship between efflux coefficients (k_{21}) determined by the DM and the GM for BSPGSH (data from Geng et al., 1995).*

with saturable uptake (BSPGSH and HA) in the GM and the DM. From the various parameter estimates of the two models, several conclusions can be drawn. The first regards the similarities between the volume for the appropriate reference in the GM and the apparent volume of distribution in the DM and among the influx constants; the second, the greater than predicted dispersion of the vascular reference curves; and the third, the influence of the large-vessel transit time delay on D_N and the rate coefficients.

Results on the fitted volumes of the vasculature (V_B) for the basic DM (set A, without t_0) were similar to those for the reference from the

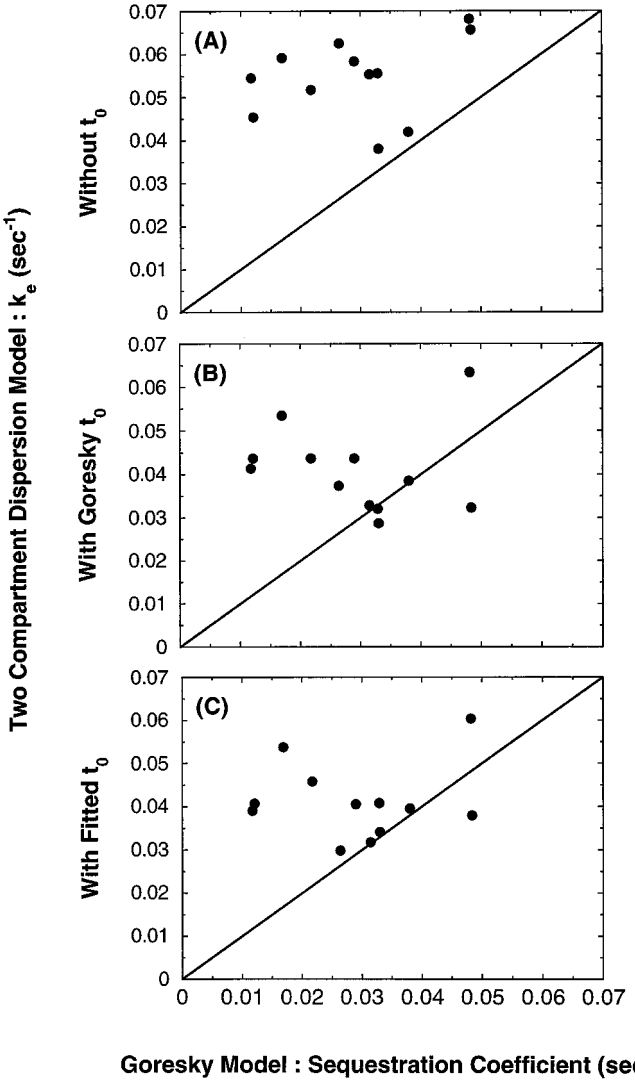

FIG. 5. *Relationship between sequestration coefficients (k_e) determined by the DM and the GM for BSPGSH (data from Geng et al., 1995).*

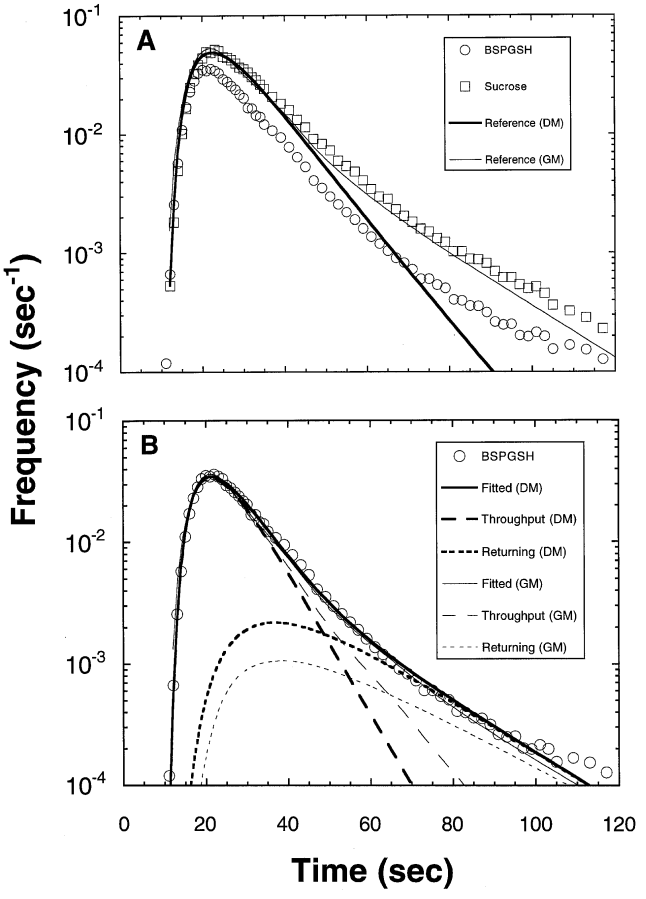

FIG. 6. *Model fit to a representative MID experiment conducted with [^{3}H]BSPGSH (214 μM).*

A, reference curves for the DM (set C) and the GM; *B*, the fitted line and throughput and returning components for the DM (set C) and the GM.

GM [$V_{Suc}(1 + \gamma_{rel})$]. The closeness of the estimates suggests that the fitted value derived from the DM provides a sound estimate of the apparent volume of distribution for the solute in the vasculature (defined as "the reference" in the GM). This volume is not the combined volumes of the sinusoidal blood and the Disse space, as originally conceived. However, the difference is expected to be small, because the apparent volume of distribution for the solute approximates the total albumin space or the total sucrose space for drugs that are totally bound or unbound to albumin, respectively. Moreover, the *a priori* assignment of V_B as 15% of the wet liver mass, as adopted in many reports (Evans *et al.*, 1991, 1993), underestimates the volume for the reference in the DM and leads to poor fits (data not shown).

The influx coefficient (k_{12}) of the DM was found to be highly correlated with that ($f_u k_1 \theta'$) of the GM (figs. 3 and 8). The observation was the result of the similarities of the respective reference curves at the early times (upswing portions of figs. 6 and 10), such that the predictions of the two models coalesced, as noted by Rowlett and Harris (1976). However, the respective reference curves eventually deviated, mostly for the later-in-time segments or the "tails" of the dilution profiles, such that the efflux and sequestration coefficients that characterize the returning component for the labeled tracer were also dissimilar. For this reason, the fit to the GM is superior (compare CD values in table 2) to that to the DM, although the fit to the DM is generally quite good, especially for the early data.

To investigate whether the large-vessel transit time could account for these differences, we included the lag time parameter t_0 in the DM, either as an assigned parameter (value of t_0 from the GM, set B) or as a fitted parameter (set C). Inclusion of t_0 in the DM (sets B and C) slightly improved the correspondence of influx, efflux, and sequestration coefficients between the DM and the GM. The most significant change occurred with D_N, which increased approximately 2–3-fold as a direct result of the incorporation of t_0 (table 2). This was also found in an analysis of the DM with closed- or mixed-boundary conditions, with or without t_0 as a fitted parameter, in rat liver-perfusion/MID studies conducted with catheters of varying lengths, in which different D_N estimates were observed for the noneliminated reference indicators in the absence of t_0 (Schwab *et al.*, 1998). The inclusion of t_0 in the DM provided a common D_N (~0.22) for the noneliminated indicators (labeled RBCs, albumin, sucrose, and water), as expected with the dispersive capability of the liver. The universality of this value provides full justification for including the time delay. The finding suggests that, after the initial delay, the same extent of dispersion exists for the noneliminated references, with a common D_N (varying from 0.16 to 0.31 among preparations), regardless of the distribution volumes or catheter sizes (Schwab *et al.*, 1998). Interestingly, the goodness of fit was also improved when t_0 was considered in the DM in the present analysis (higher values for the CD and MSC)

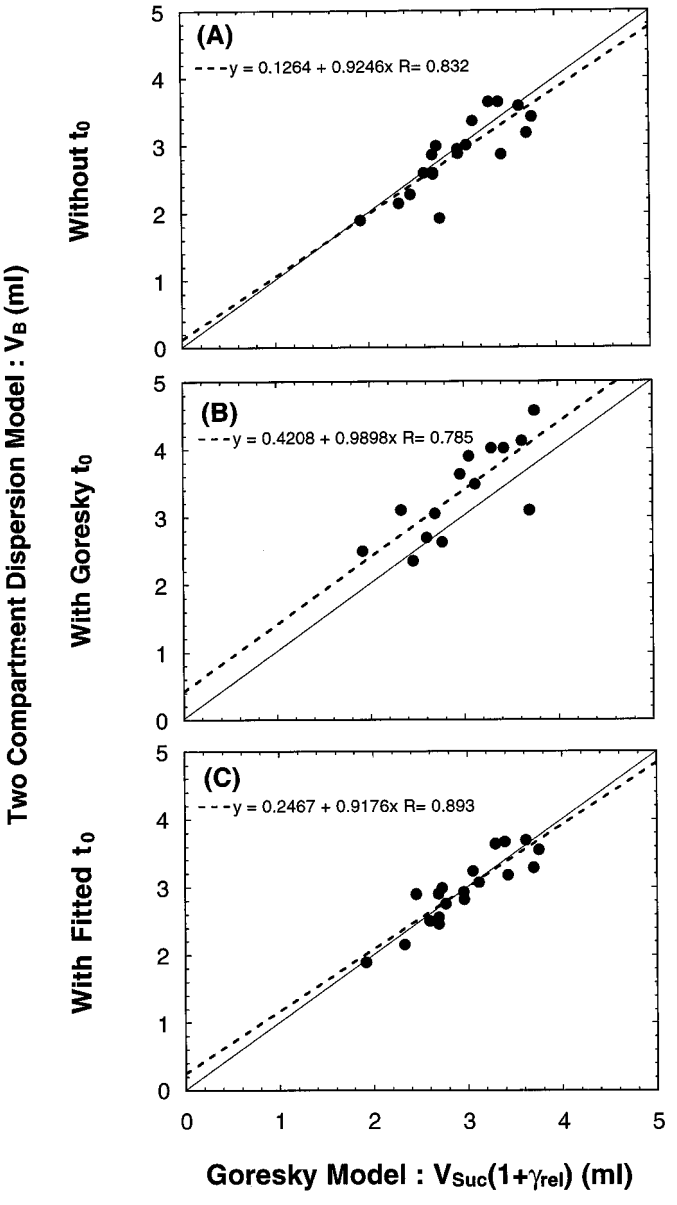

FIG. 7. *Relationship between V_B of the DM and $V_{Suc}(1 + \gamma_{rel})$ of the GM for sets A, B, and C for HA (data from Yoshimura et al., 1998).*

The *dashed lines* were established by linear regression (equations shown, with correlation coefficients, R), whereas the *solid lines* are the lines of identity.

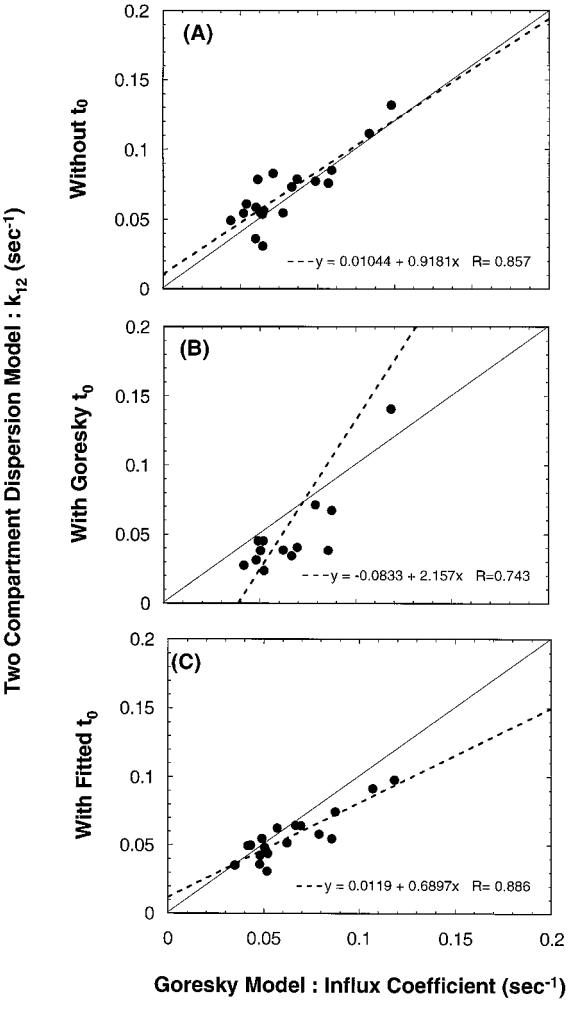

FIG. 8. *Relationship between influx coefficients (k_{12}) determined by the DM and the GM for HA (data from Yoshimura et al., 1998).*

The *dashed lines* were established by linear regression (equations shown, with correlation coefficients, R), whereas the *solid lines* are the lines of identity.

(table 2). The hypothesis that the large nonexchanging vessels would not add to the dispersion of solutes in the liver thus appears valid. Further support for the use of t_0 is provided by the excellent superposition of the curves for the diffusible noneliminated indicators onto the labeled RBC curve (scaling the time and concentration terms by the ratio of the distribution volumes) when the elapsed time is corrected for t_0 (Goresky, 1963). Audi *et al.* (1994, 1995) have demonstrated that, in the lung, virtually all of the dispersion occurs in the capillary beds and only an undetectable amount of dispersion exists in the arterial and venous trees. Taking these findings together, we conclude that the addition of t_0 for fitting is an appropriate refinement of the DM for hepatic modeling. However, there appears to be no consistent relationship for the t_0 values between the DM and the GM (fig. 11); the t_0 values for BSPGSH were quite similar for the DM and the GM, but the fitted t_0 values for the DM were consistently lower than those obtained by the superposition procedure of Goresky.

Because the large-vessel transit time could not explain the major differences in the estimates for the transfer coefficients obtained with the GM and the DM, differences in the vascular reference curves for BSPGSH or HA might be the reason for the disparities. For the DM, the reference curve is an inverse Gaussian distribution of transit times and is described by a rapid upslope followed by a monoexponential decay; for the GM, the reference curve is molded by the shapes of curves for the appropriate reference indicators, *i.e.* albumin and sucrose and their dispersions within the liver, because of the partial binding of the solute to albumin (figs. 6 and 10). It was readily apparent that the reference curves for the DM and the GM were similar at early time points but diverged after 2 or 3 MTTs. The small difference in the early reference curves reflected the similarities in estimates for k_{12} determined by the two models. Whereas the reference curve for the DM declined monoexponentially, the corresponding profile for the GM decayed in a fashion that closely resembled that of sucrose, with a slightly protracted tail. This difference in the downslopes of the reference curves brought about uncertainties in the throughput and returning components. There was lack of a definitive pattern observed for BSPGSH and HA with regard to the throughput and returning components (figs. 6 and 10). The throughput component is highly correlated with the magnitude of k_{12} and the shape and

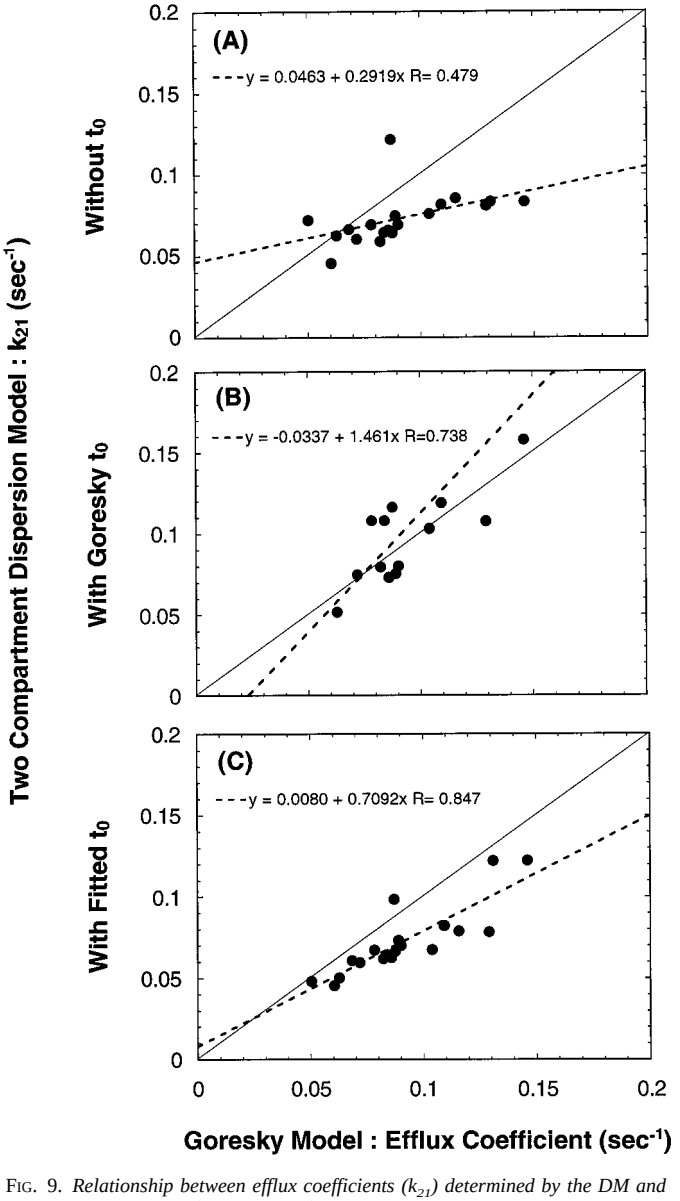

FIG. 9. *Relationship between efflux coefficients (k_{21}) determined by the DM and the GM for HA (data from Yoshimura et al., 1998).*

The *dashed lines* were established by linear regression (equations shown, with correlation coefficients, R), whereas the *solid lines* are the lines of identity.

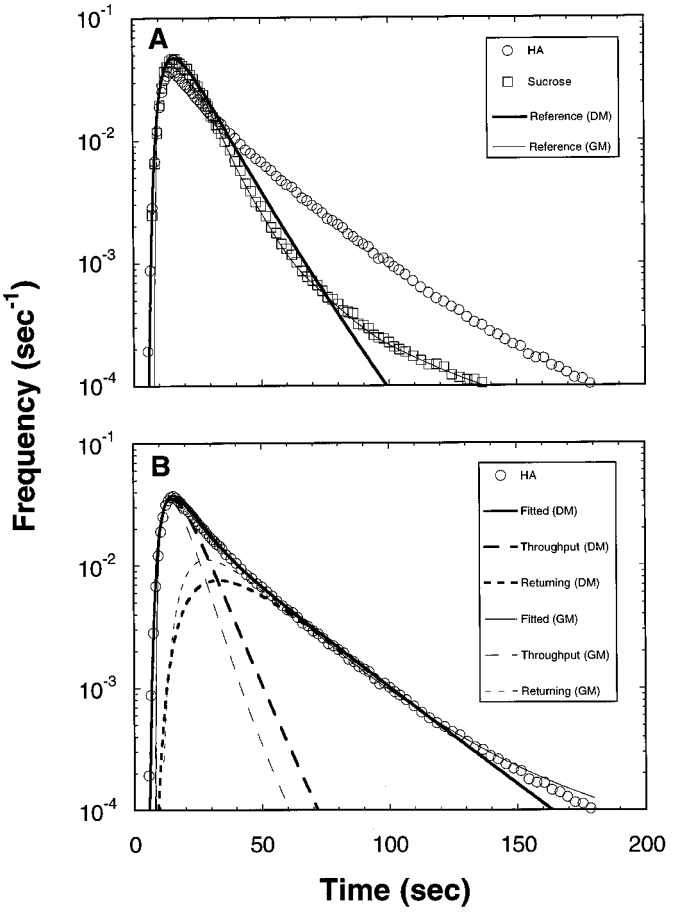

FIG. 10. *Model fit to a representative MID experiment conducted with [^{3}H]HA (930 μM).*

A, reference curves for the DM (set C) and the GM; *B*, the fitted lines and throughput and returning components for the DM (set C) and the GM.

TABLE 3

Comparison of MTT and CV^2 values between the GM and the DM for BSPGSH and HA

	BSPGSH		HA	
	MTT[a]	CV^2[b]	MTT[a]	CV^2[b]
	sec		*sec*	
GM	17.4 ± 5.4	1.10 ± 0.72	26.1 ± 3.0	1.39 ± 0.35
DM[c]	15.8 ± 4.3	0.88 ± 0.42	25.9 ± 3.1	0.87 ± 0.21
p[d]	<0.05	>0.05	>0.05	<0.0001

[a] MTT corrected for inflow and outflow catheters and large-vessel transit times.
[b] Relative variance.
[c] Two-compartment DM with fitted t_0 (set C).
[d] Paired *t* test.

downslope of the reference curve. When the estimated k_{12} for the DM is greater than that for GM, the throughput component for the DM is greater than that for the GM and, conversely, the returning component is lower. A greater disparity exists for the returning component, which is obtained as a difference curve, especially when it is small. This is manifested as highly variable estimates for k_{21} and k_e with the DM and the GM.

It must be reemphasized that, for the GM, the reference curve is constructed from the full complement of noneliminated reference indicators, and its basis should be firmly established. Comparison of the outflow profile for the diffusible labeled tracer with that for the reference would, in essence, correct for the heterogeneities in capillary transit time and account for micromixing or geometric tortuosity, as claimed by some investigators of liver physiology (King *et al.*, 1996; Weiss, 1997). The suitability of the model is apparent when the late-in-time data are well fitted and displayed in semilogarithmic plots (high CD values) (table 2). This was seldom performed with the DM for noneliminated reference indicators and the eliminated tracer solute. The late-in-time observations that highlight the dispersion within the system showed a systematic deviation from the fitted curve for the DM. For this reason, the MTT and CV^2 for the DM are underestimates (table 3).

However, in some instances, the tailing profile for tracers such as enalaprilat (Schwab *et al.*, 1990) and BSPGSH (in Eisai hyperbilirubinemic mutant rats) (Geng *et al.*, 1998) could not be explained by the present DM and GM but could be modeled by the presence of a deep intracellular pool (equivalent to three-compartment DM fitting; fits not shown). In other instances, the influence of tight intracellular binding or slow diffusion (Luxon and Weisiger, 1993; Yasui *et al.*,

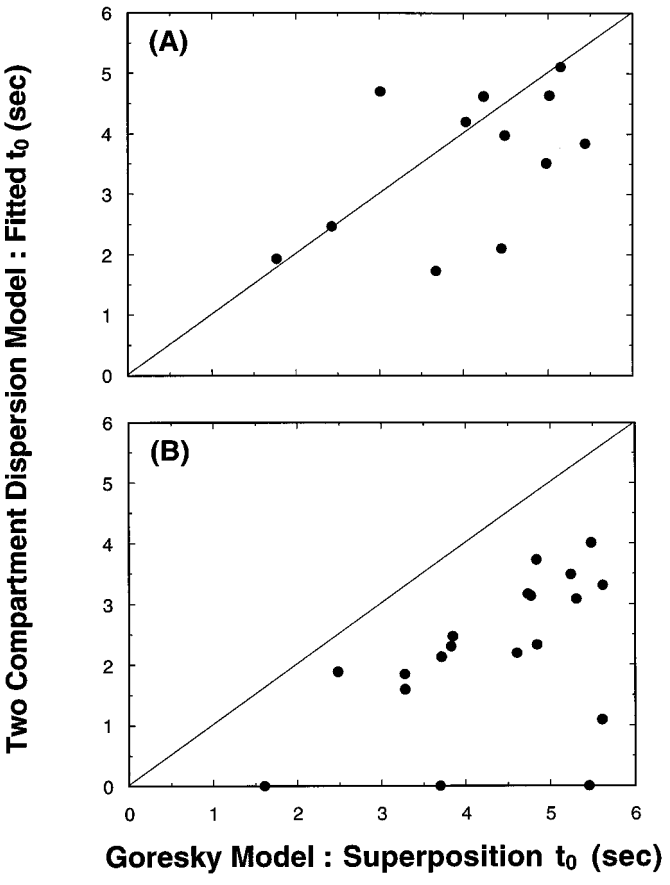

FIG. 11. *Plots of the fitted* t_0 *for the DM* vs. *the* t_0 *for the GM, obtained with the superposition procedure, for BSPGSH* (A) *and HA* (B).

1995b) could explain the unexpected RTDs of these solutes. For the DM, it should also be recognized that parameter identification was poor for efflux and removal, especially when the presence of a deep intracellular pool was evoked (fits not shown). Moreover, one must recognize the strong interrelationships between V_B and k_{12}, in addition to V_B and D_N, with the fitting procedure.

The comparison, however, reveals the utility of the DM. To reiterate a few points, DM is simpler with respect to computation and experimental strategy than the GM. The volume for the reference and the influx coefficient (and therefore uptake clearance) are well estimated, and this should provide insight into the uptake mechanism for solutes. Also, the exact amount of the dose can be verified independently using the area of the reference curve, thus circumventing experimental errors in its volumetric assessment. For optimization of the DM, however, model fitting with t_0 is necessary to provide improved estimates of V_B and k_{12}. Furthermore, proper application of tracer methodology necessitates the use of tracers in the injection dose under steady-state conditions for the bulk unlabeled compound. The appropriateness of the curve function for the sham experiment (without liver) must be demonstrated, because it is of paramount importance in the deconvolution procedure for the tracer outflow profiles. If the simple transfer function with monoexponential decay (eq. 8) were used instead of the biphasic decay curve model (eq. 12) in the analysis of the sham experiment data for the DM in the present study, D_N, V_B, and t_0 would be overestimated, whereas k_{12}, k_{21}, and k_e would be underestimated in the labeled tracer data (comparison not shown). Experimentally, it is necessary that data collection be extended beyond 3 MTTs, and it is imperative that the radiolabels quantified are identical to the quantities of the named drug or its metabolites. These recommendations ensure the proper use of indicator dilution profiles in providing mechanistic insight into drug uptake processes.

References

Audi SH, Krenz GS, Linehan JH, Rickaby DA and Dawson CA (1994) Pulmonary capillary transport function from flow-limited indicators. *J Appl Physiol* **77:**332–351.

Audi SH, Linehan JH, Krenz GS, Dawson CA, Ahlf SB and Roerig DL (1995) Estimation of the pulmonary capillary transport function in isolated rabbit lungs. *J Appl Physiol* **78:**1004–1014.

Bronikowski TA, Dawson CA and Linehan JH (1987) On indicator dilution and perfusion heterogeneity: a stochastic model. *Math Biosci* **23:**1–27.

Chou CH, Evans AM, Fornasini G and Rowland M (1993) Relationship between lipophilicity and hepatic dispersion and distribution for a homologous series of barbiturates in the isolated perfused rat liver. *Drug Metab Dispos* **21:**933–939.

Chou C-H, McLachlan AJ and Rowland M (1995) Membrane permeability and lipophilicity in the isolated perfused rat liver: 5-ethylbarbituric acid and other compounds. *J Pharmacol Exp Ther* **275:**933–940.

Danckwerts PV (1953) Continuous flow systems: distribution of residence times. *Chem Eng Sci* **2:**1–13.

Díaz-García JM, Evans AM and Rowland M (1992) Application of the axial dispersion model of hepatic drug elimination to the kinetics of diazepam in the isolated perfused rat liver. *J Pharmacokinet Biopharm* **20:**171–193.

Evans AM, Hussein Z and Rowland M (1991) A two-compartment dispersion model describes the hepatic outflow profile of diclofenac in the presence of its binding protein. *J Pharm Pharmacol* **43:**709–714.

Evans AM, Hussein Z and Rowland M (1993) Influence of albumin on the distribution and elimination kinetics of diclofenac in the isolated perfused rat liver: analysis by the impulse-response technique and the dispersion model. *J Pharm Sci* **82:**421–428.

Geng WP, Schwab AJ, Goresky CA and Pang KS (1995) Carrier-mediated uptake and excretion of bromosulfophthalein-glutathione in perfused rat liver: a multiple indicator dilution study. *Hepatology* **22:**1188–1207.

Geng W, Schwab AJ, Horie T, Goresky CA and Pang KS (1998) Hepatic uptake of bromosulfophthalein-glutathione in perfused EHBR mutant rat liver: a multiple indicator dilution study. *J Pharmacol Exp Ther* **284:**480–492.

Goresky CA (1963) A linear method for determining liver sinusoidal and extravascular volumes. *Am J Physiol* **204:**626–640.

Goresky CA, Bach GG and Nadeau BE (1973) On the uptake of materials by the intact liver: the transport and net removal of galactose. *J Clin Invest* **52:**991–1009.

Hussein Z, McLachlan AJ and Rowland M (1994) Distribution kinetics of salicylic acid in the isolated perfused rat liver assessed using moment analysis and the two-compartment axial dispersion model. *Pharm Res* **11:**1337–1345.

King RB, Raymond GM and Bassingthwaighte JB (1996) Modeling of blood flow heterogeneity. *Ann Biomed Eng* **24:**352–372.

Luxon BA and Weisiger RA (1993) Extending the multiple indicator dilution method to include slow intracellular diffusion. *Math Biosci* **113:**211–230.

Miller DL, Zanolli CS and Gumucio JJ (1979) Quantitative morphology of the sinusoids of the hepatic acinus. *Gastroenterology* **76:**965–969.

Nishimura M, Yamaoka K, Naito S and Nakagawa T (1996) Hepatic local disposition of a drug with high protein binding and high hepatic clearance using BOF-4272 as a model drug. *Biol Pharm Bull* **19:**1197–1202.

Ohata Y, Yamaoka K, Yasui H and Nakagawa T (1996) Consideration on moments of outflow profile in liver perfusion system with change in perfusate flow rate using oxacillin as model drug. *Biol Pharm Bull* **19:**83–87.

Pang KS and Rowland M (1977) Hepatic clearance of drugs. I. Theoretical consideration of a "well-stirred" model and a "parallel tube" model: influence of hepatic blood flow, plasma and blood cell binding, and the hepatocellular activity on hepatic drug clearance. *J Pharmacokinet Biopharm* **5:**625–653.

Pang KS, Sherman IA, Schwab AJ, Geng W, Barker F III, Dlugosz JA, Cuerrier G and Goresky CA (1994) Role of the hepatic artery in the metabolism of phenacetin and acetaminophen: an intravital microscopic and multiple indicator dilution study in perfused rat liver. *Hepatology* **20:**672–683.

Pang KS, Xu N and Goresky CA (1991) D_2O as a substitute for ^3H_2O, as a reference indicator in liver multiple-indicator dilution studies. *Am J Physiol* **261:**G929–G936.

Perl W and Chinard FP (1968) A convection-diffusion model of indicator transport through an organ. *Circ Res* **22:**273–298.

Roberts MS, Donaldson JD and Rowland M (1988) Models of hepatic elimination: comparison of stochastic models to describe residence time distributions and to predict the influence of drug distribution, enzyme heterogeneity, and systemic recycling on hepatic elimination. *J Pharmacokinet Biopharm* **16:**41–83.

Roberts MS and Rowland M (1985) Hepatic elimination: a dispersion model. *J Pharm Sci* **74:**585–587.

Roberts MS and Rowland M (1986) A dispersion model of hepatic elimination. 1. Formulation of the model and bolus considerations. *J Pharmacokinet Biopharm* **14:**227–260.

Rowland M, Benet LZ and Graham GG (1973) Clearance concepts in pharmacokinetics. *J Pharmacokinet Biopharm* **1:**123–136.

Rowlett RD and Harris TR (1976) A comparative study of organ models and numerical techniques for the evaluation of capillary permeability from multiple-indicator dilution data. *Math Biosci* **29:**273–298.

Schwab AJ, Barker F III, Goresky CA and Pang KS (1990) Transfer of enalaprilat across rat liver cell membranes is barrier limited. *Am J Physiol* **258:**G461–G475.

Schwab AJ, Geng W and Pang KS (1998) Application of the dispersion model for description of the outflow dilution profiles of noneliminated reference indicators in rat liver perfusion studies. *J Pharmacokinet Biopharm*, in press.

Ueda K, Yamaoka K, Rodriguez ME, Shibukawa A and Nakagawa T (1997) Enantioselective local disposition of semotiadil (*R*-enantiomer) and veosemotiadil (*S*-enantiomer) in perfused rat liver. *Drug Metab Dispos* **25:**281–286.

Weiss M (1997) A note on the interpretation of tracer dispersion in the liver. *J Theor Biol* **184:**1–6.

Winkler K, Keiding S and Tygstrup N (1973) Clearance as a quantitative measure of liver function, in *The Liver: Quantitative Aspects of Structure and Function* (Paumgartner P and Presig R eds) pp 144–155, S Karger, Basel.
Wolkoff AW, Goresky CA, Sellin JD, Gatmaitan Z and Arias IM (1979) Role of ligandin in the transfer of bilirubin from plasma into liver. *Am J Physiol* **236:**E638–E648.
Yano Y, Yamaoka K, Aoyama Y and Tanaka H (1989) Two-compartment dispersion model for analysis of organ perfusion system of drugs by fast inverse Laplace transform (FILT). *J Pharmacokinet Biopharm* **17:**179–202.
Yano Y, Yamaoka K, Minamide T, Nakagawa T and Tanaka H (1990) Evaluation of protein binding effect on local disposition of oxacillin in rat liver by a two-compartment dispersion model. *J Pharm Pharmacol* **42:**632–636.
Yano Y, Yamaoka K, Yasui H and Nakagawa T (1991) Effect of perfusion rate on the local disposition of cefixime in liver perfusion system based on two-compartment dispersion model. *Drug Metab Dispos* **19:**1022–1027.
Yasui H, Yamaoka K, Fukuyama T and Nakagawa T (1995a) Effect of liver intoxication by carbon tetrachloride on hepatic local disposition of oxacillin using moment characteristics as index. *Drug Metab Dispos* **23:**779–785.
Yasui H, Yamaoka K and Nakagawa T (1995b) New hepatocellular diffusion model for analysis of hepatobiliary transport processes of drugs. *J Pharmacokinet Biopharm* **23:**183–203.
Yoshimura T, Schwab AJ, Tao L, Barker F and Pang KS (1998) Hepatic uptake of hippuric acid, a monocarboxylic acid, and interaction with lactate and benzoate: a multiple indicator dilution, perfused rat liver study. *Am J Physiol* **274:**G10–G20.